A Kinetic Study of the Soft Metal Ion-promoted Hydrolyses of Some *S*-Acetals

By **Derek P. N. Satchell** * and **Thomas J. Weil**, Department of Chemistry, King's College, Strand, London WC2R 2LS

The *S*-acetals (III)—(VII) hydrolyse readily in aqueous ethanol or in aqueous dioxan solutions containing an excess of Tl^{3+} or Ag^+ ions to give benzophenone and the appropriate sulphide. The hydrogen-ion catalysed hydrolyses are very slow by comparison and the supposedly soft ions Cd^{2+} and Cu^{2+} have even less effect than H_3O^+. Kinetic and spectroscopic studies of the hydrolyses, mainly at 25 °C, show that the Tl^{3+}-promoted reactions occur *via* the rapid formation of a 1 Tl^{3+} : 1-*S*-acetal adduct. This adduct is formed stoicheiometrically with (IV), (V), and (VII), but in small amounts with (III) and (VI). The tripositive adduct probably reacts with water in the slow step of the overall hydrolysis. This adduct can also lose charge by proton dissociation from hydroxy groups in the bound *S*-acetal, or from thallium-bound water. The resulting dipositive adducts, however formed, hydrolyse much less rapidly than the tripositive adducts. The (chelated) dipositive adduct from (V) is sufficiently stable for contributions to hydrolysis from a [2 Tl : 1-*S*-acetal]$^{4+}$ adduct to be detected. The Ag^+-promoted hydrolyses proceed principally *via* small amounts of rapidly formed dipositive 2 Ag^+ : 1-*S*-acetal adducts. For (V), where loss of a carboxy proton can occur, the formation constant of the monopositive [2 Ag : 1-*S*-acetal]$^+$ adduct is very large (*K ca.* 10^7 l mol^{-1}) but that of the dipositive adduct is small, as for the other *S*-acetals. With (V) and (VI) the 1 Ag^+ : 1-*S*-acetal adduct is formed stoicheiometrically and with (IV) its formation constant is large (*K ca*, 900 l mol^{-1}). For (III), (IV), (VI), and (VII) these 1 : 1 adducts contribute significantly to the hydrolysis at low silver ion concentrations. For both the Tl^{3+}- and the Ag^+-promoted reactions the effects of ionic strength are consistent: where more charged adduct can form an increase in ionic strength increases the reaction rate; where adduct formation is complete, changes in ionic strength have little effect on the rate. The *S*-acetals display wide (up to 10^5-fold) differences in reactivity towards hydrolysis and their sequence of reactivity alters markedly with the promoting ion. With both ions (VI) hydrolyses relatively slowly. For all the substrates Tl^{3+} is a better promoter than Ag^+. Exact comparisons of reactivity are impossible owing to the differences in mechanistic detail and in solvent. In view of its soft acid character Tl^{3+} is surprisingly more acidic towards the *O*-containing acetals than towards those having just two S atoms. For (IV) and Ag^+ the establishment of the pre-equilibrium giving the 1 Ag^+ : 1-*S*-acetal adduct is slow enough at 25 °C to be followed by stopped-flow spectroscopy.

METAL ion-promoted hydrolyses, and related reactions, of *S*-acetals [*e.g.* equation (1)] have important applications in preparative organic chemistry, but few kinetic studies of such hydrolyses have been made.[1] So far the hydrolysis of only two types of compound, (I) and (II),

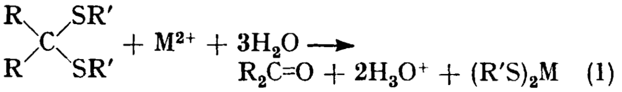

$$R_2C(SR')_2 + M^{2+} + 3H_2O \longrightarrow R_2C{=}O + 2H_3O^+ + (R'S)_2M \quad (1)$$

both *OS*-acetals, have been examined kinetically.[2,3] In both cases, the solvent was a dioxan–water mixture and the metal ion was Hg^{2+} used in conjunction with various amounts of hydrogen chloride and of potassium chloride. We report now on the hydrolyses of some other types of

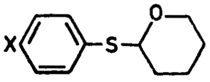

(I)

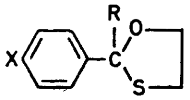

(II)

S-acetal, (III)—(VII), promoted by Tl^{3+} and by Ag^+ ions in either an ethanol–water or a dioxan–water solvent.

EXPERIMENTAL

Materials.—(a) S-*Acetals*. (i) Bis(ethylthio)diphenylmethane (III). We adapted Fieser's method [4] for use with ethanethiol. Benzophenone (5 g) was dissolved in ethanethiol (10 g) and boron fluoride–diethyl ether (10 g) added. After 10 min an oil had separated and the mixture was extracted with ether. The ether extract was washed with aqueous sodium carbonate and then with water and dried ($MgSO_4$). Removal of the ether left the crude acetal as a pungent oil.

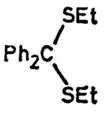

(III)

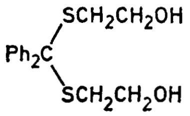

(IV)

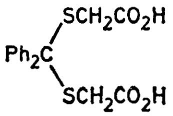

(V)

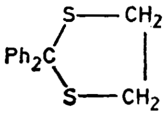

(VI)

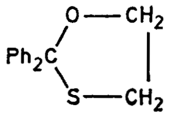

(VII)

The crude product was purified by chromatography on silica gel with light petroleum (b.p. 40—60°) as the liquid phase. The resulting oil (75%) was confirmed as (III) by microanalysis and n.m.r. spectroscopy.

(ii) 4,4-Diphenyl-3,5-dithiaheptane-1,7-diol (IV). Benzophenone and 2-mercaptoethanol can lead predominantly either to (IV) or to (VII), depending upon the reaction conditions. Diol (IV) is best prepared in the presence of an excess of the thiol. Reed and Jelineck's method [5] using hydrogen chloride as catalyst led to poor yields. Satisfactory yields (52%) of (IV) were obtained by dissolving benzophenone (5 g) in 2-mercaptoethanol (5 g) and adding boron fluoride–diethyl ether (10 g). After 30 min the precipitate formed was filtered off and recrystallised from ethanol. The crystals had m.p. 84.5 °C. The open-chain structure of the product was confirmed by microanalysis and by its n.m.r. and i.r. spectra.

(iii) 4,4-Diphenyl-3,5-dithiaheptanedioic acid (V). This compound was prepared by Ritter and Lover's method.[6] Recrystallization from ethanol gave plates, m.p. 175 °C. The product had the expected n.m.r. spectrum.

(iv) 2,2-Diphenyl-1,3-oxathiolan (VII). This compound was made, using Djerassi and Gormann's azeotropic reflux technique,[7] from benzophenone (50 g) and a deficit of 2-mercaptoethanol (14 g) with benzene (100 ml) as solvent and toluene-*p*-sulphonic acid (0.8 g) as catalyst. When most of the water had been liberated, the mixture was cooled, washed with aqueous sodium carbonate and then with water, and dried. Removal of the benzene followed by fractional distillation of the residual oil gave a cut, b.p. 161 °C at 2 Torr, which crystallized slowly to plates, m.p. 32 °C. The product was confirmed as (VII) by microanalysis and by i.r. and n.m.r. spectroscopy. It decomposed slowly at 25 °C and was stored at 0 °C.

(v) 2,2-Diphenyl-1,3-dithiolan (VI). This compound was prepared from benzophenone (2 g) and ethanedithiol (1.6 g) in the presence of boron fluoride–diethyl ether (2 g). With these reagents there is little danger of forming the open-chain derivative since the cyclic compound (VI) forms preferentially even when an excess of dithiol is present. The crude product separated after a few minutes. Recrystallization from ethanol gave needles, m.p. 95 °C. Microanalysis and the n.m.r. spectrum established the product as (VI).

(b) *Other reagents*. In the preparative work Fison's reagent grade benzophenone, ethanethiol, ethanedithiol, toluene-*p*-sulphonic acid, benzene, and diethyl ether, and B.D.H. reagent grade mercaptoethanol and mercaptoacetic acid were all used without purification. Hydrogen chloride was generated from sodium chloride and concentrated sulphuric acid. Fison's boron fluoride–diethyl ether was distilled under nitrogen before use. In the kinetic work thallium nitrate, silver perchlorate, and sodium perchlorate were B.D.H. AnalaR grade reagents, cadmium nitrate and copper nitrate were B.D.H. reagent grade materials, perchloric acid and dioxan were Fison's analytical grade reagents, and ethanol was the Burrough's u.v. grade product. These reagents, were used as such except that some batches of dioxan were further purified by distillation from sodium. Double-distilled water was used in making up reaction mixtures.

Spectroscopic Measurements.—I.r. and n.m.r. spectra were recorded using Perkin-Elmer 297 and R126 instruments, respectively. U.v. spectra were measured either with a Unicam SP 800 instrument (for scanning spectra) or with a Unicam SP 500 instrument (for measurements at a single wavelength). The latter instrument was fitted with an SP 45 scale-expander and a Vitatron VL 2001 chart recorder. U.v. cell housings were maintained at a fixed temperature, usually 25.0 ± 0.2 °C. For reactions with $t_{\frac{1}{2}} \lesssim 30$ s, u.v. measurements were made with a Durrum–Gibson D110 stopped-flow spectrophotometer fitted with improved drive syringes and thermostatting system (which permitted temperature control to within ±0.2 °C), with a stop-block and trigger-switch assembly based on Caldin's design,[8] and with modified mounts for the u.v. source (which improved focusing). The output of the stopped-flow instrument was recorded either on a Vitatron VL 2001 chart recorder (for reactions with $t_{\frac{1}{2}} > 2$ s) or on a Hewlett–Packard 1207B storage oscilloscope. All the u.v. instruments were calibrated against National Physical Laboratory approved standards.

Kinetic Arrangements.—The solvent used for the kinetic experiments with a particular substrate (see Tables) depended upon the latter's solubility. For all substrates the solvent contained at least 75% (v/v) water. Stock solutions of the various reagents were prepared and reaction mixtures made up from these by standard methods, using samples which had been brought to the required reaction temperature. For reactions with $t_{\frac{1}{2}} \gtrsim 600$ s mixtures were made up in volumetric flasks and then transferred to the spectrophotometer cell, for reactions with 60 s < $t_{\frac{1}{2}}$ < 600 s mixtures were made up directly in the SP 500 spectrophotometer cells, and for reactions with $t_{\frac{1}{2}} \lesssim 60$ s the stopped-flow technique was used. Reference cells contained all components except the *S*-acetal. In some cases runs could be conducted using either the SP 500 spectrophotometer (plus chart recorder) or the stopped-flow instrument. Good agreement (within ±10%) was observed between these two methods.

S-Acetals (III)—(VII) all lead to benzophenone on hydrolysis and the progress of all reactions was monitored by following the appearance of this product which absorbs strongly at *ca.* 254 nm. The sulphide product [see reaction (1)] also contributes significantly to absorption in this region for two of the substrates. All reaction mixtures absorbed weakly at 254 nm at the start of a run. In the metal ion-promoted reactions the metal ion concentration was always maintained in a ten or more fold excess over that of the *S*-acetal. Under these conditions all the hydrolyses are first-order processes. The observed first-order rate constants (k_{obs}) were calculated from plots of $\log(A_\infty - A_t)/(A_\infty - A_0)$ against time, where A_∞, A_t, and A_0 represent the absorbances at infinite time, at time t and at zero time, respectively. A_∞ Values were taken after about ten half-lives. In a few instances some precipitation of the metal–thiol product occurred towards the end of a run but satisfactory values of A_∞ could usually be obtained. Plots were normally rectilinear over more than three half-lives. With Ag^+, values of k_{obs} were almost always reproducible to within ±10% (often to within ±5%); with Tl^{3+}, which absorbs significantly in the region of interest and for which the majority of runs required the stopped-flow method, the reproducibility was sometimes lower, but was always within ±15%. All runs were repeated three or more times, and average values of k_{obs} calculated. For each *S*-acetal the effects on k_{obs} of changes in the concentrations of the metal ion and of the hydrogen ion (maintained with perchloric acid) were studied, as well as the effects of changes in ionic strength (maintained with sodium perchlorate). Most reaction mixtures (and all thallium nitrate stock solutions) contained added hydrogen ions; this was (a) to buffer the hydrogen ions produced in the hydrolyses [reaction(1)] and (b) to repress the ionisation of thallium-bound water and so prevent the precipitation of thallium hydroxide. Our results for the various reagent conditions and *S*-acetals are in Tables 1—11 and Figures 1—10.

Adduct Formation between Metal Ions and S-Acetals.—In a number of cases the initial absorbance A_0 measured on making up a reaction mixture, differed from that expected from the known absorbances of the reactants and therefore suggested that the *S*-acetal and metal ion had rapidly formed an adduct. When the discrepancy was sufficiently large, and when the subsequent decomposition of the adduct was not too fast to prevent accurate measurement of A_0 (if necessary by extrapolation to zero time), then the dependance of A_0 on the metal ion concentration could be studied. Sometimes an equilibrium was revealed and sometimes the complete conversion of the *S*-acetal into an adduct. In the latter cases Harvey and Manning's method [9] was used to determine the stoicheiometry of the adduct. The results of these experiments are discussed below.

Reaction Products and Stoicheiometry.—The nature of the products of the various reactions, using either Tl^{3+} or Ag^+ ions as the promoter, was examined in two ways: by preparative-scale experiments which simulated as far as possible the concentration conditions of the kinetic runs, and by comparison of the final (t_∞) spectra of reaction mixtures (from 220—400 nm) with those of artificial product mixtures prepared on the assumption of stoicheiometric reaction according to equation (1). Excellent agreement (within ±2% at all wavelengths) was always obtained in the spectral comparisons and good (>70%) yields of benzophenone were isolable in the preparative experiments. The sulphides, which can react further, were not easy to characterise as solids.

RESULTS AND DISCUSSION

Hydrogen Ion-catalysed Hydrolysis.—Results in Table 1 show that the hydrolysis of (VII) is catalysed by hydrogen ions in the absence of thallium or silver ions.

TABLE 1

The hydrogen ion-catalysed hydrolysis of *S*-acetal (VII)

$[(VII)]_{init} \simeq 5 \times 10^{-5}$M; temperature = 25.0 ± 0.2 °C; ionic strength = 1.95M; solvent = 20% (v/v) ethanol–water

$[H_3O^+]/M$	0.20	0.50	1.00	1.95
$10^4k_{obs}/s^{-1}$	0.50	1.5	2.5	5.8

This catalysed hydrolysis was not examined in detail, but (VII) was shown to be more susceptible to hydrogen ion catalysis than any of the *S*-acetals (III)—(VI). This is probably because (VII) alone contains an oxygen atom at the site of hydrolysis to which the (hard) proton can relatively easily attach itself. Compound (VII) is *ca.* 35-fold less reactive in this reaction than is the related compound 2-methyl-2-phenyl-1,3-oxathiolan (II; R = Me, X = H).[2] The hydrogen ion-catalysed hydrolysis of (VII) is negligibly slow compared with the Tl^{3+}- and Ag^+-promoted hydrolyses. The same is true for all the *S*-acetals used in this study, (III) and (VI) being especially inert towards hydrogen ions. The effects of hydrogen ions in the metal ion-promoted reactions do not therefore represent contributions from independent hydrogen ion catalysis.

TABLE 2

The thallium(III) ion-promoted hydrolysis of *S*-acetal (III)

$[(III)]_{init} \simeq 2.5 \times 10^{-5}$M; temperature = 25.0 ± 0.2 °C; solvent = 25% (v/v) dioxan–water

(i) Effect of thallium ion concentration ($[H_3O^+]$ = 0.10M; ionic strength = 0.13M)

$10^3[Tl^{3+}]/M$	0.30	0.50	1.00	2.50	3.00
k_{obs}/s^{-1}	3.1	5.1	9.9	28	30

(ii) Effect of hydrogen ion concentration ($[Tl^{3+}] = 5.0 \times 10^{-4}$M; ionic strength = 0.91M)

See Figure 1

(iii) Effect of ionic strength ($[Tl^{3+}] = 5.0 \times 10^{-4}$M; $[H_3O^+]$ = 0.01M)

Ionic strength/M	0.013	0.26	0.51	0.76	0.91
k_{obs}/s^{-1}	0.81	1.4	2.5	3.5	3.9

TABLE 3

The thallium(III) ion-promoted hydrolysis of *S*-acetal (IV)

$[(IV)]_{init} \simeq 1.0$—2.5×10^{-5}M; temperature = 25.0 ± 0.2 °C, solvent = 1% (v/v) ethanol–water

(i) Effect of thallium ion concentration ($[H_3O^+]$ = 0.50M; ionic strength = 0.8M)

$10^2[Tl^{3+}]/M$	0.05	0.10	0.25	0.50	1.50	2.50	3.75
$10^{-2}k_{obs}/s^{-1}$	3.0	3.0	2.9	3.1	3.1	2.9	3.1

(ii) Effect of hydrogen ion concentration ($[Tl^{3+}] = 5.0 \times 10^{-3}$M; ionic strength = 0.55M)

$[H_3O^+]/M$	0.05	0.10	0.125	0.25	0.375	0.50
$10^{-2}k_{obs}/s^{-1}$	0.31	0.59	0.78	1.6	2.4	3.1

(iii) Effect of ionic strength ($[Tl^{3+}] = 5 \times 10^{-3}$M; $[H_3O^+]$ = 0.10M)

Ionic strength/M	0.13	0.19	0.28	0.41	0.53
$10^{-2}k_{obs}/s^{-1}$	0.57	0.60	0.58	0.58	0.59

TABLE 4

The thallium(III) ion-promoted hydrolysis of *S*-acetal (V)

$[(V)]_{init} \simeq 10^{-4}$M; temperature = 25.0 ± 0.2 °C; solvent = 5% (v/v) ethanol–water

(i) Effect of thallium ion concentration ($[H_3O^+]$ = 0.50M; ionic strength = 0.55M)

See Figure 2

(ii) Effect of hydrogen ion concentration ($[Tl^{3+}] = 1.0 \times 10^{-3}$M; ionic strength = 0.51M)

See Figure 3

(iii) Effect of ionic strength ($[Tl^{3+}] = 1.0 \times 10^{-3}$M; $[H_3O^+]$ = 0.50M)

Ionic strength/M	0.51	1.01	1.52	2.02	2.53
$10^3k_{obs}/s^{-1}$	4.8	5.1	5.0	5.1	5.6

Thallium Ion-promoted Hydrolysis.—The pattern of results obtained with this metal ion is simpler than that found for silver ions; we therefore discuss thallium first. Our results are in Tables 2—6 and Figures 1—5. *S*-Acetals (III), (IV), (VI), and (VII) hydrolyse very rapidly in the presence of Tl^{3+} ions and required the stopped-flow technique; the acid (V) hydrolyses more slowly and could be studied using the SP 500 instrument. For (V), examination of the pre-equilibrium between

TABLE 5

The thallium(III) ion-promoted hydrolysis of *S*-acetal (VI)

$[(VI)]_{init} \simeq 2.5 \times 10^{-5}$M; temperature = 25.0 ± 0.2 °C; solvent = 25% (v/v) dioxan–water

(i) Effect of thallium ion concentration ($[H_3O^+]$ = 0.50M; ionic strength = 0.53M)

See Figure 5

(ii) Effect of hydrogen ion concentration ($[Tl^{3+}] = 5.0 \times 10^{-4}$M; ionic strength = 0.95M)

$[H_3O^+]/M$	0.05	0.15	0.30	0.55	0.95
$10k_{obs}/s^{-1}$	0.60	1.3	1.3	1.3	1.3

(iii) Effect of ionic strength ($[Tl^{3+}] = 5.0 \times 10^{-4}$M; $[H_3O^+]$ = 0.05M)

Ionic strength/M	0.053	0.15	0.30	0.55	0.95
$10k_{obs}/s^{-1}$	0.04	0.10	0.20	0.29	0.60

TABLE 6

The thallium(III) ion-promoted hydrolysis of *S*-acetal (VII)

$[(VII)]_{init} \simeq 2.5 \times 10^{-5}$M; temperature = 25.0 ± 0.2 °C, solvent = 20% (v/v) ethanol–water

(i) Effect of thallium ion concentration ($[H_3O^+]$ = 0.25M; ionic strength = 0.28M)

$10^3[Tl^{3+}]$/M	0.50	0.75	1.0	2.0	3.0	5.0
k_{obs}/s^{-1}	15	15	16	15	15	16

(ii) Effect of hydrogen ion concentration ($[Tl^{3+}] = 5.0 \times 10^{-4}$M; ionic strength = 0.93M)

$10[H_3O^+]$/M	0.25	0.75	1.25	2.75	5.25	7.75	9.25
k_{obs}/s^{-1}	6.3	13	21	25	25	26	26

(iii) Effect of ionic strength ($[Tl^{3+}] = 5.0 \times 10^{-4}$M; $[H_3O^+]$ = 0.025M)

Ionic strength/M	0.08	0.13	0.28	0.53	0.93
k_{obs}/s^{-1}	5.4	5.7	6.1	6.3	6.3

Tl^{3+} and *S*-acetal by Harvey and Manning's method showed that a 1 Tl^{3+} : 1 *S*-acetal adduct is formed stoicheiometrically over a wide concentration range and that in all the kinetic experiments (V) was present effectively completely as the 1 : 1 adduct (Figure 4).

Three effects were observed, depending upon the substrate, when the thallium ion concentration was varied at fixed values of the hydrogen ion concentration and of the ionic strength: (a) a plot of k_{obs} against $[Tl^{3+}]$ was rectilinear and passed through the origin [substrates (III) and (VI), Figure 5], (b) the plot was rectilinear but had an intercept on the k_{obs} axis [(V), Figure 2], and (c) k_{obs} was independent of $[Tl^{3+}]$ [(IV) and (VII)]. Where k_{obs} is independent of $[Tl^{3+}]$ changes in ionic strength have little effect on the value of k_{obs} whereas in other cases k_{obs} increases rectilinearly with ionic strength. The effects of increases in hydrogen ion concentration, at fixed values of the thallium ion concentration and of the ionic strength, are two-fold: (a) there is, probably for all substrates, a rapid, equilibrium-like increase in k_{obs} to a maximum value reached at $[H_3O^+]$ *ca.* 0.15M, and (b) this increase is followed either by a further rectilinear increase in k_{obs} {which largely conceals the increase at low values of $[H_3O^+]$; substrates (IV) and (V)} or by a region where k_{obs} is

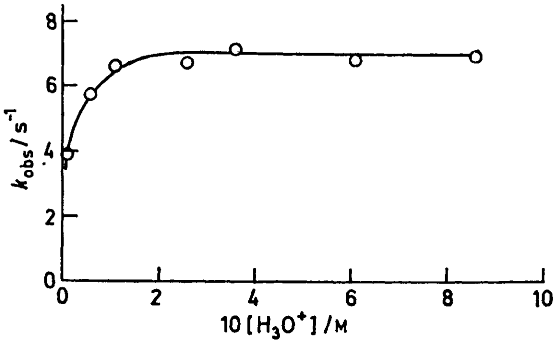

FIGURE 1 Effect of hydrogen ion concentration in the Tl^{3+} ion-promoted hydrolysis of (III) ($[Tl^{3+}]$ 5.0×10^{-4}M; ionic strength 0.91M)

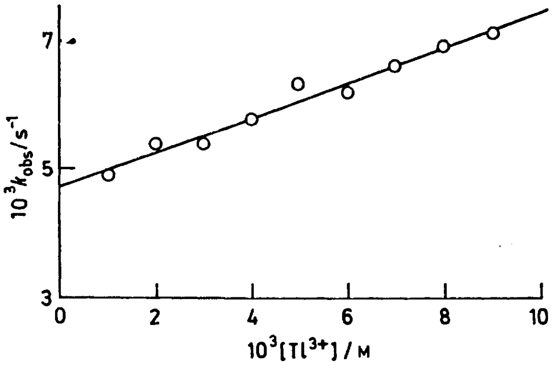

FIGURE 2 Effect of thallium ion concentration in the hydrolysis of (V) ($[H_3O^+]$ 0.50M; ionic strength 0.55M)

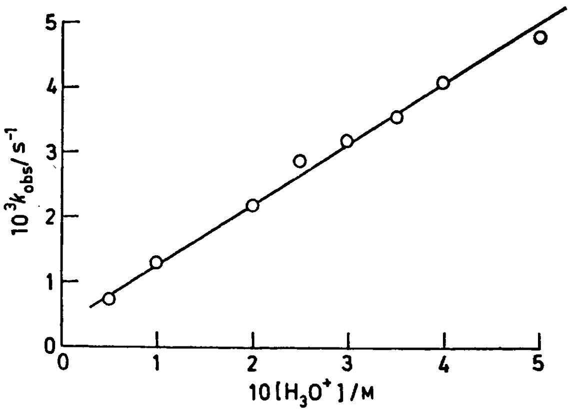

FIGURE 3 Effect of hydrogen ion concentration in the Tl^{3+} ion-promoted hydrolysis of (V) ($[Tl^{3+}]$ 10^{-3}M; ionic strength 0.51M)

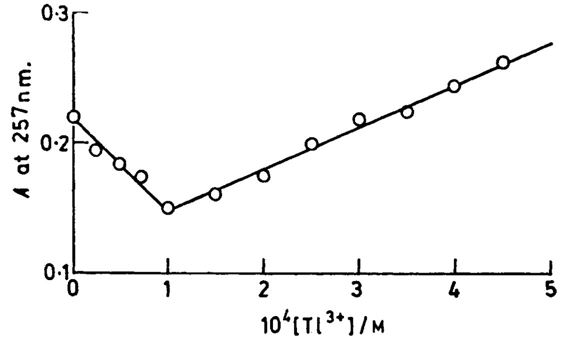

FIGURE 4 Adduct formation between (V) and Tl^{3+} ions. Harvey and Manning plot {[(V)] 10^{-4}M; $[H_3O^+]$ 0.05M; temperature 25.0 ± 0.2 °C}

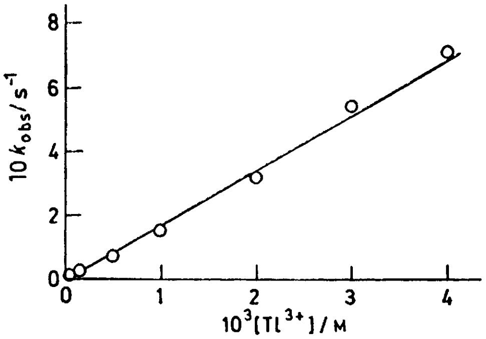

FIGURE 5 Effect of thallium ion concentration in the hydrolysis of (VI) ($[H_3O^+]$ 0.50M; ionic strength 0.53M)

independent of $[H_3O^+]$ [(III), (VI), and (VII); Figure 1].

These various findings are compatible, as will be shown below, with the outline mechanism given in Scheme 1.

$$[Tl(H_2O)_n]^{3+} + H_2O \rightleftharpoons [Tl(OH)(H_2O)_{n-1}]^{2+} + H_3O^+ \qquad \text{Fast, (2)}$$

$$[Tl(H_2O)_n]^{3+} + S\text{-acetal} \rightleftharpoons \underset{\text{(VIII)}}{[(H_2O)_{n-1}Tl \leftarrow S\text{-acetal}]^{3+}} + H_2O \qquad \text{Fast, (3)}$$

$$\text{(VIII)} + H_2O \rightleftharpoons \underset{\text{(IX)}}{[H_2O)_{n-2}(HO)Tl \leftarrow S\text{-acetal}]^{2+}} + H_3O^+ \qquad \text{Fast, (4)}$$

For *S*-acetals with an ionisable proton [*S*-acetal–OH, compounds (IV) and (V)] another hydrogen ion-dependent equilibrium (5) is possible.

$$\text{(VIII)} + H_2O \rightleftharpoons \underset{\text{(X)}}{[H_2O)_{n-1}Tl \leftarrow S\text{-acetal}{-}O]^{2+}} + H_3O^+ \qquad \text{Fast, (5)}$$

$$\text{(X)} + [Tl(OH)(H_2O)_{n-1}]^{2+} \rightleftharpoons \underset{\text{(XI)}}{[2Tl : 1\text{-}S\text{-acetal adduct}]^{4+}} \qquad \text{Fast, (6)}$$

$$\text{(VIII)} + x\,H_2O\ (?) \longrightarrow \text{Products} \qquad \text{Slow, (7)}$$

$$\text{(XI)} + x\,H_2O\ (?) \longrightarrow \text{Products} \qquad \text{Slow, (8)}$$

SCHEME 1

Equilibrium (2) is known [10] to lie to the left when $[H_3O^+] \gtrsim 0.1$M; the same is therefore probably true for equilibrium (4). The conversion of the various $[Tl(OH)]^{2+}$ species into $[Tl(H_2O)]^{3+}$ species, in equilibria (2) and (4), as $[H_3O^-]$ is increased therefore very probably underlies the effects of hydrogen ion concentration on k_{obs} at $[H_3O^+] \lesssim 0.15$M when these are the only effects observed [*S*-acetals (III), (VI), and (VIII); *e.g.* Figure 1]. Our results therefore suggest that the reactivity of dipositive species such as (IX) in subsequent hydrolysis steps is small compared with the reactivity of the tripositive species (VIII). For substrates (IV) and (V) the acid ionisation equilibrium (5) is also possible. We suggest that, when present, this equilibrium lies well to the right at all hydrogen ion concentrations studied, so that only a small concentration of the tripositive species (VIII) is present and this concentration is proportional to $[H_3O^+]$. If (VIII) is much more reactive than (X) this circumstance will explain the hydrogen ion dependance of k_{obs} for compounds (IV) and (V) (Figure 3) and also be consistent with the foregoing conclusions concerning the relative reactivities towards hydrolysis of species (VIII) and (IX).

The dependance of k_{obs} on $[Tl^{3+}]$ was always studied at values of $[H_3O^+]$ where equilibrium (2), and therefore probably also (4), lies well to the left; species (IX) can be ignored under these circumstances. To account for the effect of changes in $[Tl^{3+}]$ on k_{obs} for *S*-acetal (III) we assume that in this case equilibrium (3) lies far to the left; the concentration of (VIII) is then proportional to $[Tl^{3+}]$ and, since there is no chance of species (X) and (XI) for this substrate, the rate of hydrolysis will be first-order in the thallium ion concentration, as found. A similar situation applies for *S*-acetal (VI). For these two *S*-acetals, at $[H_3O^+] \gtrsim 0.15$M, Scheme 1 reduces to Scheme 2. The rate $= -d[S\text{-acetal}]/dt = -d[\text{(VIII)}]/dt = k_7[\text{(VIII)}] = K_3k_7[Tl^{3+}][S\text{-acetal}] = k_{obs}[S\text{-acetal}]$, where $k_{obs} = K_3k_7[Tl^{3+}] = k[Tl^{3+}]$, as found experimentally.

$$[Tl(H_2O)_n]^{3+} + S\text{-acetal} \rightleftharpoons \text{(VIII)} \qquad \text{Fast, } K_3\ (3)$$

$$\text{(VIII)} + x\,H_2O\ (?) \longrightarrow \text{Products} \qquad \text{Slow, } k_7\ (7)$$

SCHEME 2

Although increases in $[H_3O^+]$ above 0.15M have no effect on k_{obs} for (III) and (VI), an increase in ionic strength does increase k_{obs} (Tables 2 and 5); this is presumably because the value of K_3 and/or of k_7 is increased.

For *S*-acetal (VII), when $[H_3O^+] \gtrsim 0.15$M, Scheme 2 is again applicable except that equilibrium (3) is now taken to lie far to the right, effectively all the *S*-acetal being present as (VIII). This assumption leads to the especially simple rate equation: rate $= k_7[S\text{-acetal}] = k_{obs}[S\text{-acetal}]$, with k_{obs} independent of both $[H_3O^+]$ and $[Tl^{3+}]$, as found (Table 6). For this *S*-acetal, changes in ionic strength have little effect on k_{obs}. This fact suggests that k_7 is little affected by the ionic strength and that the effects found for (III) and (VI), noted above, arise from changes in the value of K_3 (*i.e.* for those substrates more adduct is formed at high ionic strength).

The values of k_{obs} for *S*-acetal (IV) are, like those for (VII), independent of $[Tl^{3+}]$. Again therefore we assume that equilibrium (3) lies well to the right and that (VIII) is formed stoicheiometrically. For (IV), however, the further possibility exists of the engagement of the adduct (VIII) in equilibrium (5) to give (X). If equilibrium (5) also lies well to the right then, since the dipositive (X) is likely to be less reactive towards hydrolysis than (VIII), an increase in $[H_3O^+]$ will be expected to lead to an increase in k_{obs}, [(VIII)] being proportional to $[H_3O^+]$ under such conditions. Here then, for $[H_3O^+] \gtrsim 0.15$M, Scheme 1 reduces to Scheme 3.

$$[Tl(H_2O)_n]^{3+} + S\text{-acetal} \rightleftharpoons \text{(VIII)} \qquad \text{Fast, (3)}$$

$$\text{(VIII)} + H_2O \rightleftharpoons \text{(X)} + H_3O^+ \qquad \text{Fast, } K_5\ (5)$$

$$\text{(VIII)} + x\,H_2O\ (?) \longrightarrow \text{Products} \qquad \text{Slow, } k_7\ (7)$$

SCHEME 3

For Scheme 3 the rate $= -d[S\text{-acetal}]/dt = -d[\text{(VIII)}]/dt = k_7[\text{(VIII)}] = k_7[\text{(X)}][H_3O^+]/K_5 = (k_7/K_5)[H_3O^+][S\text{-acetal}] = k_{obs}[S\text{-acetal}]$ with $k_{obs} = (k_7/K_5)[H_3O^+] = k'[H_3O^+]$, as found. This analysis assumes a negligible decomposition *via* (X). Changes in ionic strength again have little effect on k_{obs} and therefore probably do not much affect K_5. The reason for this, and for the unreactivity of (X) towards hydrolysis, presumably lies in the structure of (X) (see below).

For *S*-acetal (V) the effects are more complicated than for the other four substrates dealt with above: (V) is the only substrate for which, at $[H_3O^+] \gtrsim 0.15$M, there is an increase in k_{obs} both for increase in $[Tl^{3+}]$ and for increase in $[H_3O^+]$, although the effect of $[Tl^{3+}]$ is relatively minor (Figure 2). We also know from the Harvey and Manning plot (Figure 4) that the 1 : 1 adduct (VIII) is formed stoicheiometrically. It appears therefore that more than one thallium ion can be associated with this *S*-acetal and we suggest equilibrium (6), since it seems more likely that $[Tl(OH)(H_2O)_{n-1}]^{2+}$ will be involved here than $[Tl(H_2O)_n]^{3+}$. For (V) the full Scheme 1 is therefore needed with equilibria (2) and (4) lying well left at $[H_3O^+] \lesssim 0.15\text{M}$, with equilibrium (3), and probably also (5), lying well to the right, and with equilibrium (6) assumed to lie to the left. Such conditions lead to equation (9). At any fixed value of $[H_3O^+]$, equation (9)

$$\text{Rate} = k_{obs}[S\text{-acetal}] = \{(k_7/K_5)[H_3O^+] + k_8K_6K_2[Tl^{3+}]/[H_3O^+]\}[S\text{-acetal}] \quad (9)$$

correctly predicts the form of the dependence of k_{obs} on $[Tl^{3+}]$ (Figure 2) and for $[Tl^{3+}] = 10^{-3}\text{M}$, when $(k_7/K_5)[H_3O^+] \gg k_8K_2K_6[Tl^{3+}]/(H_3O^+]$ (see Figure 2), it predicts that $k_{obs} \simeq k[H_3O^+]$, as found experimentally.

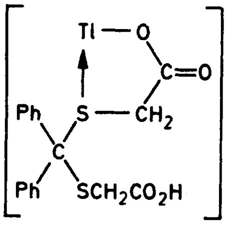

(XII)

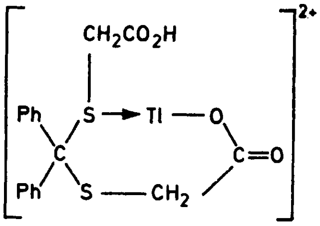

(XIII)

Assuming that the interpretation of these reactions which we have given above is in essence correct, certain other interesting conclusions can be drawn, for instance, that Tl^{3+} forms more stable complexes with acetals (IV), (V), and (VII), which contain an O and an S atom, than with acetals (III) and (VI) which contain only two S atoms. Presumably chelate complexes are involved, especially as with (IV) and (V) concomitant ionisation of an *O*-bround proton occurs, the resulting dipositive adducts (X) being particularly stable towards hydrolysis.

TABLE 7

The silver(I) ion-promoted hydrolysis of *S*-acetal (V)

$[(V)]_{init} \simeq 1.25$—$2.50 \times 10^{-5}\text{M}$; temperature = 25.0 ± 0.2 °C, solvent = 5% (v/v) ethanol–water

(i) Effect of silver ion concentration ($[H_3O^+] = 0.50\text{M}$; ionic strength = 0.51M)

See Figure 6

(ii) Effect of hydrogen ion concentration ($[Ag^+] = 5.0 \times 10^{-4}\text{M}$; ionic strength = 0.51M)

See Figure 7

(iii) Effect of ionic strength ($[Ag^+] = 5.0 \times 10^{-4}\text{M}$; $[H_3O^+] = 5.0 \times 10^{-2}\text{M}$)

Ionic strength/M	0.05	0.10	0.50	1.00
$10^4k_{obs}/s^{-1}$	5.8	6.0	6.6	7.0

The structures of these latter adducts are uncertain: they may involve a five- or a seven-membered ring [*e.g.* (XII) and (XIII)]. In view of the evidence for the formation of a 2 Tl : 1-*S*-acetal adduct (XI) with (V), we favour structure (XII). That Tl^{3+} should prefer *S*-acetal (VII) to either (III) or (VI) is unexpected. It is also interesting that all the dipositive adducts, however formed [*i.e.* as examples of (IX) or (X)], are so much less reactive than their tripositive analogues that they make a negligible contribution to k_{obs} and it is not easy to quantify their reactivity from our data. The most reactive tripositive adduct (VIII) is probably that formed by the diol (IV).

Arguing by analogy with the mercury ion-promoted hydrolysis [2] of (II) and the silver ion-promoted reactions discussed below, we consider that the slow steps (7) and (8) in Scheme 1 probably involve one or more water

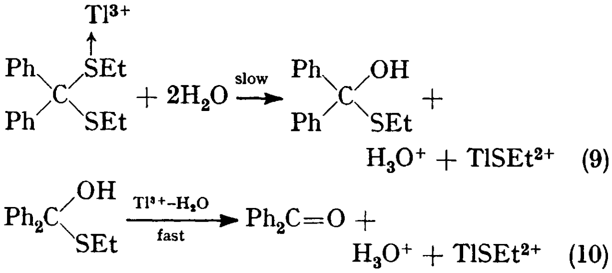

(9)

(10)

molecules. Our observations suggest, as is commonly found, that the hydrolysis of the intermediate hemiacetal is fast compared with that of the parent acetal. For (III) the product-forming steps can therefore be outlined as (9) and (10).

TABLE 8

The silver(I) ion-promoted hydrolysis of *S*-acetal (III)

$[(III)]_{init} \simeq 10^{-5}\text{M}$; temperature = 25.0 ± 0.2 °C, solvent = 25% (v/v) dioxan–water

(i) Effect of silver ion concentration ($[H_3O^+] = 5.0 \times 10^{-2}\text{M}$; ionic strength = 0.10M)

See Figure 8

(ii) Effect of hydrogen ion concentration ($[Ag^+] = 5.0 \times 10^{-3}\text{M}$; ionic strength = 0.91M)

$[H_3O^+]/\text{M}$	0.0050	0.20	0.41	0.81
k_{obs}/s^{-1}	9.8	8.5	9.3	9.9

(iii) Effect of ionic strength ($[Ag^+] = 5.0 \times 10^{-3}\text{M}$; $[H_3O^+] = 5.0 \times 10^{-3}\text{M}$)

Ionic strength/M	0.050	0.11	0.21	0.41	0.81	0.91
k_{obs}/s^{-1}	2.8	3.5	4.8	6.2	9.0	9.8

Silver Ion-promoted Hydrolysis.—With silver ions four of the five *S*-acetals showed broadly similar kinetic behaviour, whilst the other, acid (V), behaved very differently. Generally the silver ion-promoted hydro-

TABLE 9

The silver(I) ion-promoted hydrolysis of *S*-acetal (IV)

$[(IV)]_{init} \simeq 2.5 \times 10^{-5}\text{M}$; solvent = 1% (v/v) ethanol–water

(i) Effect of silver ion concentration ($[H_3O^+] = 0$; ionic strength = $5.0 \times 10^{-2}\text{M}$; temperature = 25.0 ± 0.2 °C)

$10^3[Ag^+]/\text{M}$	0.25	0.50	0.75	1.00	1.50	2.00	5.00
$10^2k_{obs}/s^{-1}$	0.018	0.065	0.13	0.18	0.32	0.42	1.0
$10^3[Ag^+]/\text{M}$	7.50	10.0	15.0	20.0	25.0	30.0	40.0
$10^2k_{obs}/s^{-1}$	1.2	3.8	7.2	14	20	28	42
$10^3[Ag^+]/\text{M}$	50.0						
$10^2k_{obs}/s^{-1}$	55						

(ii) Effect of hydrogen ion concentration ($[Ag^+] = 2.5 \times 10^{-3}\text{M}$; ionic strength = 0.90M; temperature = 25.0 ± 0.2 °C)

$[H_3O^+]/\text{M}$	0.0	0.1	0.2	0.4	0.6
$10^2k_{obs}/s^{-1}$	3.3	3.3	3.2	3.3	3.5

(iii) Effect of ionic strength ($[Ag^+] = 2.5 \times 10^{-3}\text{M}$; $[H_3O^+] = 0$; temperature = 25.0 ± 0.2 °C)

Ionic strength/M	0.0025	0.10	0.20	0.40	0.60	0.80	0.90
$10^2k_{obs}/s^{-1}$	0.17	0.67	1.1	1.6	2.7	3.2	3.5

(iv) Effect of temperature ($[Ag^+] = 5.0 \times 10^{-3}\text{M}$; $[H_3O^+] = 0$; ionic strength = 0.20M)

$T\ (\pm 0.2)/K$	283.2	298.2	303.2	313.2	323.2	328.2
$10^2k_{obs}/s^{-1}$	0.89	1.1	1.5	1.7	2.1	2.3

lyses proceeded very slowly compared with the thallium ion reactions. The rates with the two ions were most similar for compounds (III) and (V). Our results are in Tables 7—11 and Figures 6—10. We deal with (V) first.

TABLE 10

The silver(I) ion-promoted hydrolysis of *S*-acetal (VI)

$[(VI)]_{init} \simeq 5.0 \times 10^{-5}$M; solvent = 25% (v/v) dioxan–water

(i) Effect of silver ion concentration ($[H_3O^+]$ = 0.95M; ionic strength = 1.05M)

(a) At 25.0 ± 0.2 °C

$10^2[Ag^+]$/M	2.5	5.0	7.5	9.5
$10^4k_{obs}/s^{-1}$	1.1	2.9	4.5	5.8

(b) At 60.0 ± 1.0 °C

$10^2[Ag^+]$/M	0.05	0.10	0.25	0.50	0.75	1.0	5.0
$10^4k_{obs}/s^{-1}$	0.33	0.36	0.44	0.47	0.64	1.2	14

$10^2[Ag^+]$/M	7.5
$10^4k_{obs}/s^{-1}$	25

(ii) Effect of hydrogen ion concentration ($[Ag^+]$ = 0.10M; ionic strength = 1.7M; temperature = 60.0 ± 1.0 °C)

$[H_3O^+]$/M	0	0.05	0.10	0.50	1.0	1.6
$10^4k_{obs}/s^{-1}$	39	39	44	47	44	47

(iii) Effect of ionic strength ($[Ag^+]$ = 0.10M, $[H_3O^+]$ = 0; temperature = 60.0 ± 1.0 °C)

Ionic strength/M	0.10	0.20	0.30	0.60	1.1	1.7
$10^4k_{obs}/s^{-1}$	15	17	18	23	31	39

TABLE 11

The silver(I) ion-promoted hydrolysis of *S*-acetal (VII)

$[(VII)]_{init} \simeq 2.5 \times 10^{-5}$M; temperature = 25.0 ± 0.2 °C; solvent = 20% (v/v) ethanol–water

(i) Effect of silver ion concentration ($[H_3O^+]$ = 0.05M; ionic strength = 0.15M)

$10^2[Ag^+]$/M	0.05	0.10	0.25	0.50	0.75	1.0	2.5
$10k_{obs}/s^{-1}$	0.012	0.033	0.095	0.14	0.32	0.48	2.5

$10^2[Ag^+]$/M	5.0	7.5	10.0
$10k_{obs}/s^{-1}$	12	23	31

(ii) Effect of hydrogen ion concentration ($[Ag^+] = 5.0 \times 10^{-3}$M; ionic strength = 0.90M)

$[H_3O^+]$/M	0.0	0.10	0.25	0.35	0.75	0.90
$10k_{obs}/s^{-1}$	0.40	0.40	0.40	0.40	0.43	0.40

(iii) Effect of ionic strength ($[Ag^+] = 5.0 \times 10^{-3}$M; $[H_3O^+]$ = 0)

Ionic strength/M	0.10	0.25	0.50	0.75	0.90
$10k_{obs}/s^{-1}$	0.11	0.18	0.27	0.37	0.40

For (V), absorbance measurements of reaction mixtures at zero time revealed the presence of a rapidly formed Ag^+–*S*-acetal adduct. Measurements using a series of solutions with fixed *S*-acetal and hydrogen ion concentrations, but with varying silver ion concentration, indicated the existence of equilibrium (11) with K_{11} *ca.* 2.0×10^7 l^2 mol^{-2} at $[H_3O^+]$ 0.50M and ionic strength 0.51M. The fit of the data to a 1 : 1 stoicheiometry for

$$2\,Ag^+ + S\text{-acetal} \rightleftharpoons 2:1\text{-adduct}\ K_{11} \quad (11)$$

the adduct was much less satisfactory. Kinetic study (Table 7) of the hydrolysis also revealed (and independently) a dependence of k_{obs} on $[Ag^+]$ suggestive of the formation of a 2 Ag : 1-*S*-acetal adduct which becomes stoicheiometric at $[Ag^+] \gtrsim 10^{-3}$M (Figure 6). At relatively high silver ion concentrations, changes in ionic strength have little effect on k_{obs} values, but an increase in $[H_3O^+]$ leads to a rectilinear increase in k_{obs}. At $[H_3O^+] \lesssim 0.01$M the promoted hydrolysis is relatively slow but detectable (Figure 7).

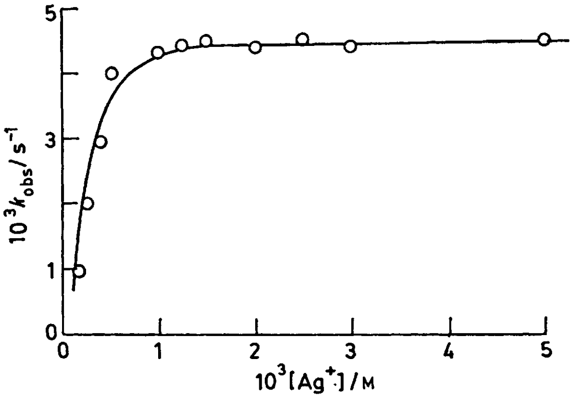

FIGURE 6 Effect of silver ion concentration in the hydrolysis of (V) ($[H_3O^+]$ 0.50M; ionic strength 0.51M)

In contrast to thallium ion promotion, dissociation of protons from silver-bound water molecules is probably not involved,[10] so that the effects of changes in $[H_3O^+]$ on k_{obs} are likely to reflect proton dissociation from the metal-bound *S*-acetal. This circumstance, our various findings and the realisation that the 2 : 1-adduct can

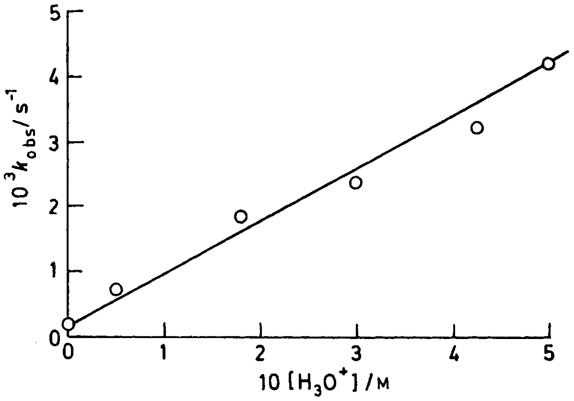

FIGURE 7 Effect of hydrogen ion concentration in the Ag^+ ion-promoted hydrolysis of (V) ($[Ag^+]$ 5.0×10^{-4}M; ionic strength 0.51M)

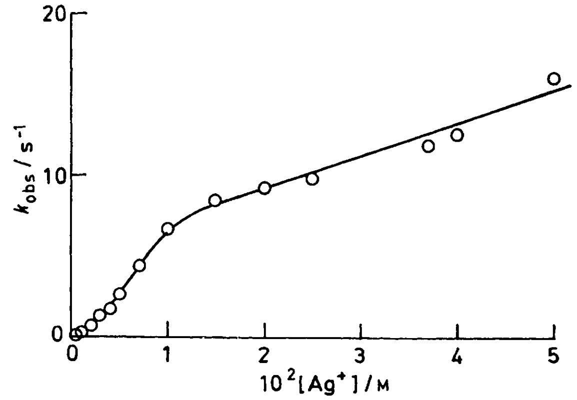

FIGURE 8 Effect of silver ion concentration in the hydrolysis of (III) ($[H_3O^+]$ 5.0×10^{-2}M; ionic strength 0.10M)

exist in various forms [*e.g.* (XIV) to (XVII) and others], lead us to suggest Scheme 4 for the silver ion-promoted hydrolysis of (V).

In Scheme 4 we assume that the 2 : 1-adduct exists principally as (XVI), or as its equivalent (XIX), and that

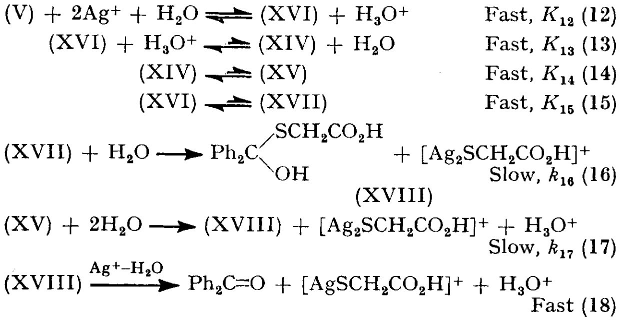

$$\text{(V)} + 2\text{Ag}^+ + \text{H}_2\text{O} \rightleftharpoons \text{(XVI)} + \text{H}_3\text{O}^+ \qquad \text{Fast, } K_{12} \quad (12)$$

$$\text{(XVI)} + \text{H}_3\text{O}^+ \rightleftharpoons \text{(XIV)} + \text{H}_2\text{O} \qquad \text{Fast, } K_{13} \quad (13)$$

$$\text{(XIV)} \rightleftharpoons \text{(XV)} \qquad \text{Fast, } K_{14} \quad (14)$$

$$\text{(XVI)} \rightleftharpoons \text{(XVII)} \qquad \text{Fast, } K_{15} \quad (15)$$

$$\text{(XVII)} + \text{H}_2\text{O} \longrightarrow \underset{\text{(XVIII)}}{\text{Ph}_2\text{C}\begin{smallmatrix}\text{SCH}_2\text{CO}_2\text{H}\\ \text{OH}\end{smallmatrix}} + [\text{Ag}_2\text{SCH}_2\text{CO}_2\text{H}]^+ \qquad \text{Slow, } k_{16} \quad (16)$$

$$\text{(XV)} + 2\text{H}_2\text{O} \longrightarrow \text{(XVIII)} + [\text{Ag}_2\text{SCH}_2\text{CO}_2\text{H}]^+ + \text{H}_3\text{O}^+ \qquad \text{Slow, } k_{17} \quad (17)$$

$$\text{(XVIII)} \xrightarrow{\text{Ag}^+\text{–H}_2\text{O}} \text{Ph}_2\text{C=O} + [\text{AgSCH}_2\text{CO}_2\text{H}]^+ + \text{H}_3\text{O}^+ \qquad \text{Fast} \quad (18)$$

SCHEME 4

all its other forms, including any neutral forms such as (XX), have much lower concentrations. With these assumptions:

$$\begin{aligned} -\text{d}[\text{(V)}]/\text{d}t &= k_{\text{obs}}[\text{(V)}]_{\text{total}} \\ &= k_{16}[\text{(XVII)}] + k_{17}[\text{(XV)}] \end{aligned}$$

Since $[\text{(V)}]_{\text{total}} \simeq [\text{(V)}] + [\text{(XVI)}] = [\text{(V)}](1 + K_{12}[\text{Ag}^+]^2/[\text{H}_3\text{O}^+])$ while $[\text{(XV)}] = K_{12}K_{13}K_{14}[\text{Ag}^+]^2[\text{(V)}]$ and $[\text{(XVII)}] = K_{12}K_{15}[\text{Ag}^+]^2/[\text{H}_3\text{O}^+]$

$$\therefore k_{\text{obs}} = \frac{(k_{16}K_{12}K_{15}/[\text{H}_3\text{O}^+] + k_{17}K_{12}K_{13}K_{14})[\text{Ag}^+]^2}{(1 + K_{12}[\text{Ag}^+]^2/[\text{H}_3\text{O}^+])} \quad (19)$$

Equation (19) is in agreement with experiment: (i) at fixed silver ion and low hydrogen ion concentrations, when the terms 1 and $k_{17}K_{12}K_{13}K_{14}$ can be ignored, it predicts a limiting value of $k_{\text{obs}} = k_{16}K_{15}$ (*ca.* 1.7×10^{-4} s^{-1}, Figure 7), (ii) at high silver ion and hydrogen ion concentrations, when $k_{16}K_{12}K_{15}/[\text{H}_3\text{O}^+] \ll k_{17}K_{12}K_{13}K_{14}$, it predicts another limiting value of $k_{\text{obs}} = k_{17}K_{13}K_{14}[\text{H}_3\text{O}^+]$ (*ca.* 45×10^{-4} s^{-1} at $[\text{H}_3\text{O}^+] = 0.50$M, Figure 6), and (iii) at a high, fixed value of $[\text{H}_3\text{O}^+]$, equation (19) can be written as $k_{\text{obs}} = a[\text{Ag}^+]^2/(1 + b[\text{Ag}^+]^2)$; the continuous line in Figure 6 is a plot of this equation with $a = 8.33 \times 10^4$ and $b = 1.85 \times 10^7$, the points being the experimental values. Since $b = K_{12}/[\text{H}_3\text{O}^+]$ this analysis gives $K_{12} = 0.93 \times 10^7$ l mol^{-1}, a value in good agreement with that calculated from the spectroscopic measurements (see above) from which $K_{12} = K_{11}[\text{H}_3\text{O}^+] = 10^7$ l mol^{-1}. Scheme 4 therefore seems justified and indeed good reasons underlie its assumptions: (a) the adduct is unlikely to exist mainly as a neutral species since previous experience[1] of silver ion promotion involving sulphur substrates shows that such an adduct would be likely to be very unreactive towards hydrolysis and, in any event, would be expected to lead to kinetic terms in $[\text{H}_3\text{O}^+]^2$, as well as in $[\text{H}_3\text{O}^+]$, since a dipositive species is going to be the most reactive; (b) (XV) and (XVII) are likely to be the species most readily decomposed by water, although (XIV) and (XVI) will be more abundant, since good evidence[1] suggests that kinetic terms in $[\text{Ag}^+]^2$ in silver ion-promotion reflect the formation of adducts in which both silver ions are attached to a single S atom.

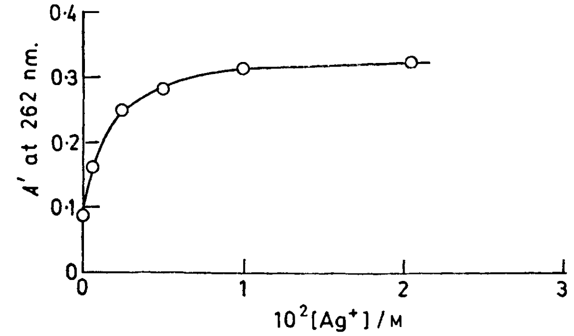

FIGURE 9 Adduct formation between silver ions and (IV) {[(IV)] 2.5×10^{-5}M; $[\text{H}_3\text{O}^+]$ 0; ionic strength 0.05M; temperature 25 ± 0.2 °C}

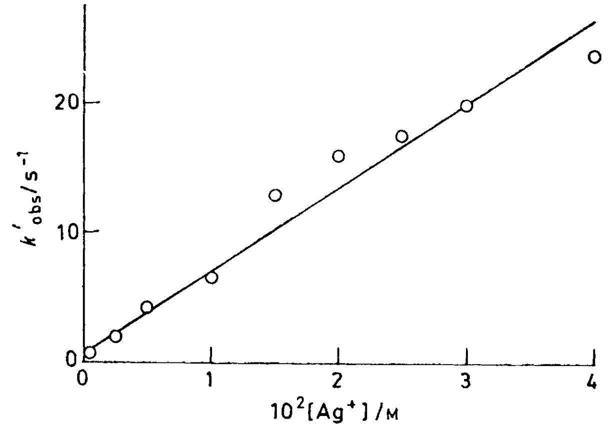

FIGURE 10 Plot of equation (32) (conditions as for Figure 9)

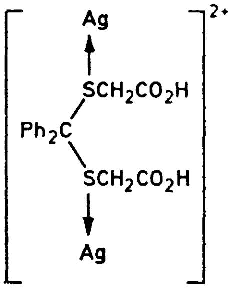

(XIV)

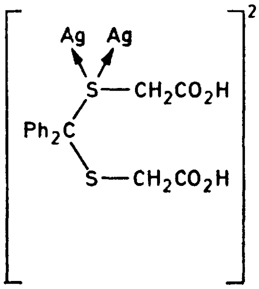

(XV)

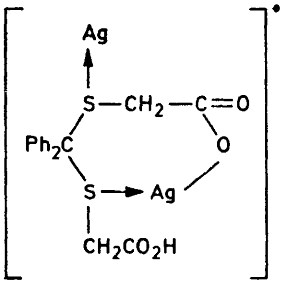

(XVI)

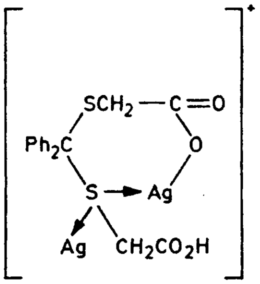

(XVII)

The remaining *S*-acetals can be considered together. For them all k_{obs} is independent of $[H_3O^+]$ (Tables 8—11). This is true even for (IV) which has two OH protons, one of which is significantly dissociated in the Tl^{3+} adduct (see above). For them all k_{obs} is approximately rectilinearly related to the ionic strength. For the thallium ion promotion this latter behaviour was observed when hydrolysis proceeded importantly *via* a charged adduct whose concentration increases at high ionic strengths. Finally for all these remaining *S*-acetals we find a rather similar dependence (*e.g.* Figure 8) of k_{obs} on $[Ag^+]$. Compound (VI) shows the simplest behaviour: at 25 °C k_{obs} is approximately proportional to $[Ag^+]$. Compound (VI) is hydrolysed more slowly by silver ion promotion than any of the other *S*-acetals and of this group is the only substrate to exhibit stoicheiometric formation of a 1 Ag^+ : 1-*S*-acetal adduct at 25 °C, even at low silver ion concentrations (as shown by Harvey and Manning's experiments.) For (VI) the outline mechanism of hydrolysis is probably that in Scheme 5, only the 2 : 1-adduct undergoing hydrolysis. Since, at 25 °C, [Ag←*S*-acetal]$^+$ $\simeq$ $[(VI)]_{total}$, this Scheme leads to equation (24), which is in agreement with experiment.

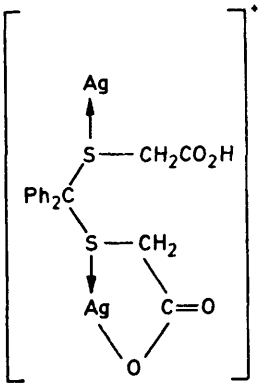

(XIX)

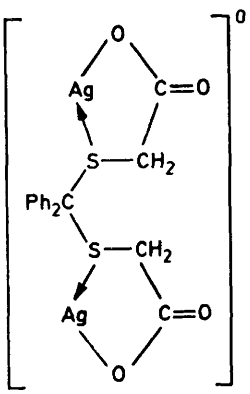

(XX)

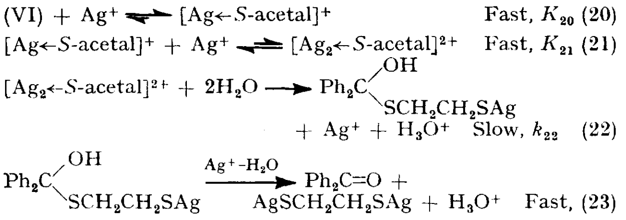

$$(VI) + Ag^+ \rightleftharpoons [Ag\leftarrow S\text{-acetal}]^+ \qquad \text{Fast, } K_{20} \quad (20)$$

$$[Ag\leftarrow S\text{-acetal}]^+ + Ag^+ \rightleftharpoons [Ag_2\leftarrow S\text{-acetal}]^{2+} \qquad \text{Fast, } K_{21} \quad (21)$$

$$[Ag_2\leftarrow S\text{-acetal}]^{2+} + 2H_2O \longrightarrow Ph_2C\begin{smallmatrix}OH\\SCH_2CH_2SAg\end{smallmatrix} + Ag^+ + H_3O^+ \qquad \text{Slow, } k_{22} \quad (22)$$

$$Ph_2C\begin{smallmatrix}OH\\SCH_2CH_2SAg\end{smallmatrix} \xrightarrow{Ag^+\text{-}H_2O} Ph_2C{=}O + AgSCH_2CH_2SAg + H_3O^+ \qquad \text{Fast, } (23)$$

SCHEME 5

$$k_{obs} = k_{22}K_{21}[Ag^+] \qquad (24)$$

Two further points are of interest for this *S*-acetal. First, because of its slow rate of hydrolysis, experiments were conducted at 60 °C, as well as at 25 °C. The dependence of k_{obs} on $[Ag^+]$ at 60 °C is much more like that found for the other three *S*-acetals of this group, (III), (IV), and (VII), at 25 °C. This suggests (see below) that the 1 : 1-adduct is not formed stoicheiometrically for (VI) at 60 °C. Secondly, we have here a substrate which forms the 1 : 1-adduct more readily than do (III), (IV), or (VII), yet is hydrolysed more slowly. This may be because the cyclic structure of (VI) confers extra stability on a chelated adduct (XXI), so that in the 2 Ag^+ : 1-*S*-acetal adduct it is more difficult for both Ag^+ ions to become wholly associated with just one S atom, which is probably the condition necessary for rapid hydrolysis (see above). This idea is supported by the fact that (VII), which is also cyclic but which forms a 1 : 1-adduct less easily (presumably because it cannot form such a stable chelate) is hydrolysed in the presence of silver ions much more rapidly than is (VI). Our results as a whole, for both thallium and silver ion promotion, suggest that the ease of decomposition of the adduct is more important than how much of it is formed.

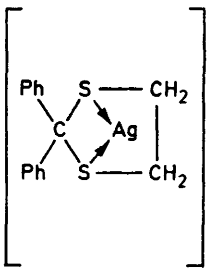

(XXI)

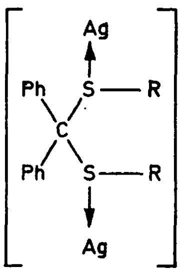

(XXIV)

The behaviours of (III), (IV), and (VII) are qualitatively compatible with Scheme 5 if equilibrium (20) does not lie so far right and if the 1 : 1-adduct has some reactivity. In the modified mechanism (Scheme 6) we assume that (XXIII) has both silver ions on the same S atom. The existence of other 2 Ag^+ : 1-*S*-acetal adducts [*e.g.* (XXIV)], provided that they are formed in low concentrations relative to (XXII) and are unreactive relative to (XXIII) towards hydrolysis, as is likely, will not much affect the kinetic pattern. Scheme 6, in which contributions to hydrolysis from these other adducts is ignored as a first approximation, leads to equation (31). That this equation can successfully reproduce the general form of the dependence of k_{obs} on $[Ag^+]$ is shown for compound (III) in Figure 8; the

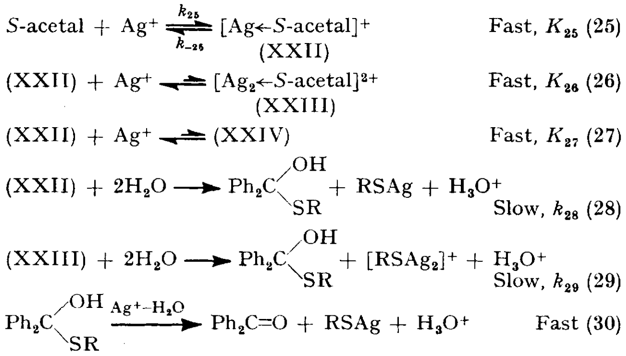

$$S\text{-acetal} + Ag^+ \underset{k_{-25}}{\overset{k_{25}}{\rightleftharpoons}} \underset{(XXII)}{[Ag\leftarrow S\text{-acetal}]^+} \qquad \text{Fast, } K_{25} \quad (25)$$

$$(XXII) + Ag^+ \rightleftharpoons \underset{(XXIII)}{[Ag_2\leftarrow S\text{-acetal}]^{2+}} \qquad \text{Fast, } K_{26} \quad (26)$$

$$(XXII) + Ag^+ \rightleftharpoons (XXIV) \qquad \text{Fast, } K_{27} \quad (27)$$

$$(XXII) + 2H_2O \longrightarrow Ph_2C\begin{smallmatrix}OH\\SR\end{smallmatrix} + RSAg + H_3O^+ \qquad \text{Slow, } k_{28} \quad (28)$$

$$(XXIII) + 2H_2O \longrightarrow Ph_2C\begin{smallmatrix}OH\\SR\end{smallmatrix} + [RSAg_2]^+ + H_3O^+ \qquad \text{Slow, } k_{29} \quad (29)$$

$$Ph_2C\begin{smallmatrix}OH\\SR\end{smallmatrix} \xrightarrow{Ag^+\text{-}H_2O} Ph_2C{=}O + RSAg + H_3O^+ \qquad \text{Fast} \quad (30)$$

SCHEME 6

$$k_{obs} = \frac{k_{28}K_{25}[Ag^+] + k_{29}K_{25}K_{26}[Ag^+]^2}{\{1 + K_{25}[Ag^+] + (K_{25}K_{26} + K_{25}K_{27})[Ag^+]^2\}} \qquad (31)$$

continuous line is based on $k_{28}K_{25} = 3.3$ l mol^{-1} s^{-1}, $k_{29}K_{25}K_{26} = 1.7 \times 10^3$ l^2 mol^{-2} s^{-1}, $K_{25} = 100$ l mol^{-1} and $K_{25}(K_{26} + K_{27}) = 5 \times 10^3$ l^2 mol^{-2}. These values, and the assumption that $K_{27} \gg 4\ K_{26}$, give $k_{28} = 3.3 \times 10^{-2}$ s^{-1} and $k_{29} \gg 1.7$ s^{-1}. These figures are therefore compatible with the assumed greater reactivity of (XXIII) compared with (XXII). The calculated value of K_{25} is, however, smaller than might be expected by comparison with the position of the 1 : 1 equilibrium for (VI) [equation (20)]. And in a similar analysis of the data for (IV) a much smaller value of K_{25} is obtained than that which can be observed directly using spectroscopic measurements (see below). Scheme 6 is therefore too simple to explain completely the complex dependences of k_{obs} on [Ag$^+$] for *S*-acetals (III), (IV), and (VII) and our calculations suggest that a small concentration of very reactive 3 Ag$^+$: 1-*S*-acetal adduct may be contributing to the hydrolysis. Further analysis appears, however, unjustified; Scheme 6 seems almost certainly along the correct general lines.

Experiments at different temperatures, especially with (IV), the second most reactive substrate with Ag$^+$, led to values of $\Delta H^\ddagger$ *ca.* 4 kcal mol^{-1} and $\Delta S^\ddagger$ *ca.* −45 cal K^{-1} mol^{-1} for the silver-promoted hydrolysis (Table 9). The small value of $\Delta H^\ddagger$ presumably arises owing to opposing effects of temperature on pre-equilibria and on the slow product-forming steps. Previous studies of soft metal ion promotion suggest that large, negative values of $\Delta S^\ddagger$ are associated with bimolecular slow steps involving water.[1]

Kinetics of Adduct Formation.—As for a number of other metal ion–*S*-acetal combinations mentioned above, reaction mixtures containing the diol (IV) and silver ions displayed a rapid increase in absorbance, before significant hydrolysis occurred, indicative of initial adduct formation. For mixtures of (IV) with Ag$^+$ the rate of this initial adduct formation was slow enough to be within the compass of the stopped-flow spectrophotometer. For a series of reaction mixtures containing a fixed concentration of (IV), but different concentrations of Ag$^+$ ions, the absorbances *A*′, measured after the initial adduct formation had occurred, revealed the presence of an equilibrium such as (25) with $K_{25} = 900 \pm 90$ l mol^{-1} (Figure 9). The subsequent hydrolysis was sufficiently slow at most silver ion concentrations for *A*′ to be obtained using the SP 500 instrument. The adduct has a maximum absorbance at 262 nm where $\varepsilon_{(\text{IV})} = 3.6 \times 10^3$ and $\varepsilon_{1\,:\,1\text{-adduct}} = 1.3 \times 10^4$. Measurements of k'_{obs}, the first-order rate constant for the approach to equilibrium, fitted equation (32), appropriate for equilibrium (25), in which k_{25} and k_{-25} represent the forward and reverse rate constants, respectively (Figure 10). At 25 °C we find $k_{25} = 750 \pm 80$ l mol^{-1} s^{-1} and

$$k'_{\text{obs}} = k_{25}[\text{Ag}^+] + k_{-25} \qquad (32)$$

$k_{-25} = 0.84 \pm 0.14$ s^{-1}. Hence $K_{25} = k_{25}/k_{-25} \simeq 900$ l mol^{-1}, a value in good agreement with that obtained independently from the *A*′ values. The significance of this moderately slow substitution at silver by (IV) is discussed in our preliminary report of this work.[11]

Cadmium(II) *and Copper*(II) *Ions as Promoters of Hydrolysis*.—Experiments using these ions revealed that if they are active at all they are less so than the hydrogen ion in the present systems. This result is in keeping with several previous studies of these ions with other sulphur compounds.[1] It seems that the class B character of these ions can be remarkably feeble.

Comparison with Previous Work.—De and Fedor[2] studied the mercury(II) ion-promoted hydrolysis of (II; R = X = H), a compound closely related to our (VII). Free Hg^{2+} ions normally have at least the soft acidity of Tl^{3+} ions.[1] However, all De and Fedor's reaction mixtures contained substantial concentrations of added chloride ions which convert Hg^{2+} ions into other mercury species (*e.g.* HgCl$_2$, HgCl$_3^-$, *etc.*) of much lower soft acidity than free Hg^{2+} ions.[1] It is doubtless for this reason that in their systems only a small fraction of the *S*-acetal is converted into an adduct with the metal species whereas in our experiments, which employed the free ions Tl^{3+} and Ag$^+$, the *S*-acetal (VII) is, under most concentration conditions, very largely converted into the 1 : 1-adduct (see above).

[9/1852 *Received*, 21*st November*, 1979]

REFERENCES

[1] D. P. N. Satchell, *Chem. Soc. Rev.* 1977, **6**, 345.
[2] N. C. De and L. R. Fedor, *J. Amer. Chem. Soc.*, 1968, **90**, 7266.
[3] L. R. Fedor and B. S. R. Murty, *J. Amer. Chem. Soc.*, 1973, **95**, 8407.
[4] L. F. Fieser and M. Fieser, ' Reagents for Organic Synthesis,' Wiley, New York, 1967, pp. 356, 643.
[5] E. E. Reid and A. Jelinek, *J. Org. Chem.*, 1950, **15**, 448.
[6] J. J. Ritter and M. J. Lover, *J. Amer. Chem. Soc.*, 1952, **74**, 5576.
[7] C. Djerassi and J. M. Gorman, *J. Amer. Chem. Soc.*, 1954, **76**, 3704.
[8] E. F. Caldin, J. E. Crooks, and A. Queen, *J. Phys.* (*E*), 1973, **6**, 930.
[9] A. E. Harvey and D. L. Manning, *J. Amer. Chem. Soc.*, 1950, **72**, 4488.
[10] L. G. Sillen and A. E. Martell, ' Stability Constants,' Chem. Soc. Special Publications Nos. 17 and 25, The Chemical Society, London, 1965 and 1971.
[11] D. P. N. Satchell and T. J. Weil, *Inorg. Chim. Acta*, 1978, **29**, L239.